Lipoyl-Homotaurine Derivative Reverts Oxaliplatin-induced Neuropathy and Reduces Cancer Cells Malignancy by Inhibiting Carbonic Anhydrase IX (CAIX).

Marco. Fragai, [¥,ʃ] Giuseppina Comito,[§] Lorenzo Di Cesare Mannelli,[#] Roberta Gualdani,[¥] Vito Calderone,[¥,ʃ] Alexandra Louka,[ʃ] Barbara Richichi,[¥] Oscar Francesconi,[¥] Andrea Angeli, [#]Alessio Nocentini,[#] Paola Gratteri,[#] Paola Chiarugi,[§] Carla Ghelardini,[d] Francesco Tadini Buoninsegni,[¥] Claudiu T. Supuran[#]* and Cristina Nativi[¥,^]*

[¥] Department of Chemistry, University of Florence, via della Lastruccia 3-13, 50019 Sesto F.no (FI) Italy.

[ʃ] CERM, University of Florence, via L. Sacconi, 6 50019 Sesto F.no (FI) Italy.

[§] Department of Exp. and Clinical Biomed. Sciences, University of Florence, V.le Morgagni, 50 50134 Firenze, Italy.

[#] Department NEUROFARBA, University of Florence, V. le Pieraccini, 6 50134 Firenze, Italy;

[^] FioGen, via L. Sacconi,6 50019 Sesto F.no (FI) Italy.

ABSTRACT Oxaliplatin (OXA) is valuable and largely used chemotherapic known to induce a neuropathy, probably the most difficult to treat. The lipoyl-homotaurine derivative, **ADM_12**, reverts *in vivo* OXA-induced neuropathy and is an effective antagonist of the nociceptive sensor channel TRPA1. Unprecedentedly, this safe analgesic was successfully tested in tests of inhibition of CA IX, a relevant therapeutic target, clearly interfering pancreatic cancer cells aggressiveness.

INTRODUCTION

The number of cancer patients is increasing worldwide and a large majority of them receive antitumoral chemotherapy. The development of new and effective anticancer drugs has extended the survival of tumor-bearing hosts, conceivably raising the proportion of patients having experienced chemotherapy-induced neuropathy (CIN).[1] CIN is considered one of the most disabling and invalidating disease affecting cancer patients: CIN induces or worsen depression, insomnia and distress, greatly affecting the quality of life and often becoming the treatment-limiting issue in the cancer therapy.[2,3] Therapeutically, CIN is still considered an intractable problem. As a matter of fact, no pharmacological treatments have demonstrated efficacy in the prevention or therapy of CIN. Mixtures of opioids and non-opioids, including vitamins and mineral salts, are generally administrated with scarce or no evidence of efficacy confirming CIN the major concern for both cancer patients and oncologists.[4] Manifestations and causes of CIN can vary substantially from drug to drug. A distinct, and probably one of the most difficult to treat, is the neuropathy induced by oxaliplatin (OXA). Mechanical and cold allodynic sensation in hands and feet are the painful effects produced which, surprisingly, may worsen after OXA administration has finished.[2] Thus, the availability of safe and effective analgesic drugs for the

treatment of chronic CIN is a task of primary importance as well as an urgent need. Acute and chronic peripheral neuropathies associated with the use of OXA have extensively been reported[5] and related to the remodeling and alteration in the expression of transient receptors potential (TRP) Ca^{2+} channels. In particular, thermo sensitive transient receptors potential Vanilloid 1 (TRPV1) and Ankyrin 1 (TRPA1) are up regulated and hyper sensitized, mediating OXA-evoked cold and mechanical allodynia.[6,7] We recently reported about the TRPA1 antagonist **ADM_09** (Figure 1),[8] which effectively reverts neuropathic pain evoked by OXA, without eliciting the negative side-effects generally observed in neuropathic pain treatment. Preserving the α-lipoic portion, which characterizes **ADM_09**, we have also reported a second lipoic-containing TRPA1 antagonist, namely **ADM_12** (Figure 1), successfully assayed to treat in vivo another orphan pain, that is the orofacial pain.[9]
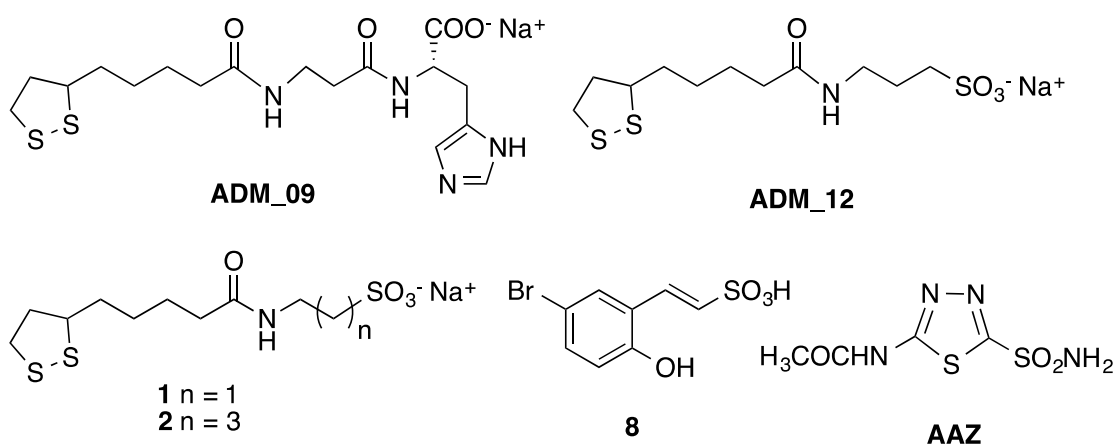

Figure 1. Structure of **ADM_09**, **ADM_12**, compounds **1**, **2**, **8** and acetazolamide (**AAZ**).

With respect to **ADM_09**, **ADM_12** presents the lipoic acid portion linked to an homotaurine and is characterized by a terminal sulfonic acid residue.[9] In a recent paper describing the inhibitory activity of a bromophenol sulfonic acid *vs.* human (*h*) carbonic anhydrases (*h*CAs, EC 4.2.1.1) implicated in cancer progression,[10] some of us proved the involvement of the sulfonic

acid residue in the binding to the CA IX active site by anchoring to the zinc-coordinated water molecule. Keeping this in mind and capitalizing on data we previously reported for **ADM_12**, we reasoned that **ADM_12** might be an excellent candidate for both the treatment of neuropathic pain induced by OXA and as a new inhibitor of CAs. Hence, we report herein on the investigation of **ADM_12**, and the corresponding homologues **1** and **2** (Figure 1) in: *a)* the treatment of OXA-induced neuropathy (OXAIN), *b)* binding tests vs. CA IX and CA XII as well as c) in CA IX-mediated cancer cells motility tests. Unprecedentedly, our data showed the double role of **ADM_12** as analgesic but also as modulator in cancer cells invasiveness.

RESULTS

Synthesis. Following the synthetic strategy reported for **ADM_12**,[9] its homologous **1** and **2** were obtained in two steps reacting the commercially available (±) α-lipoic acid with N-hydroxysuccinimide in tetrahydrofuran (THF) as solvent and in the presence of dicyclohexylcarbodiimide (DCC) to give the activated lipoic derivative **3** (Scheme 1). The unreacted DCC and the dicyclohexyl urea formed during the reaction, were removed by crystallization and pure **3** was treated with taurine **4** or with the amino sulfonic acid **5** in H_2O/DMF to afford, after purification, **1** (60%) or **2** (80%) respectively. As reported for **1** and **2** (see Scheme 1), the lipoic-containing alcohol **7**, used as control (see below), was obtained by reacting **3** with the amino alcohol **6** (Supporting Information). After purification, **7** was isolated as a yellow waxy solid in 60% yield.
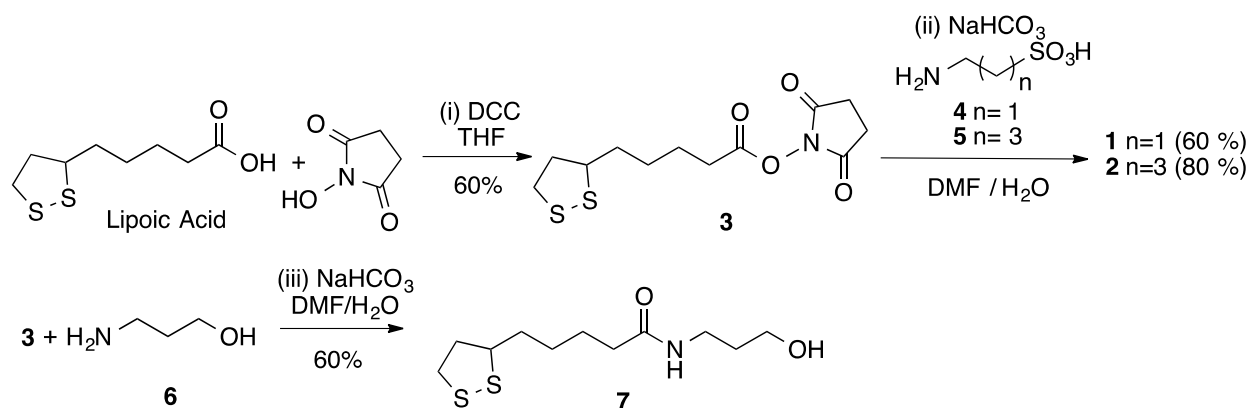
Scheme 1. Synthesis of lipoic-containing derivatives **1**, **2** and **7**

Antioxidative properties. As widely reported,[11,12] acute and chronic neurotoxicities associated with the use of OXA are related to the oxidative stress caused by this chemotherapic. Therefore, the antioxidant profile of **ADM_12** and compounds **1** and **2** was evaluated. We measured the oxidation *in vitro* of nitro blue tetrazolium (NBT) after 30 min, in the absence and in the presence of an increasing concentration of **ADM_12** (Table S2, Supporting Information). The superoxide anion (O_2^-) generated by the hypoxanthine–xanthine oxidase system increased the oxidized NBT level from 100 (basal) to about 4000 A.U. In the presence of **ADM_12** in the reaction mixture, the oxidation of NBT was inhibited in a concentration-dependent manner taking effect starting from 10 μM. The highest concentration (1000 μM) allowed to obtain a complete prevention of oxidation. Similar results were obtained testing **1** and **2** but, differently from **ADM_12**, they were not able to fully prevent the oxidation (Supporting Information). The antioxidative properties were also tested in cell culture of primary rat cortical astrocytes, a cell type strongly involved in OXA-dependent neuropathy.[13,14] A 4 h long cell treatment with 100μM OXA induced a significant, SOD-inhibitable, superoxide anion increase as evaluated by the cytochrome C assay (Figure 2A). The co-incubation with 100μM **ADM_12** or **1** or **2** inhibited the O_2^- formation by about 75% in comparison to the untreated culture.
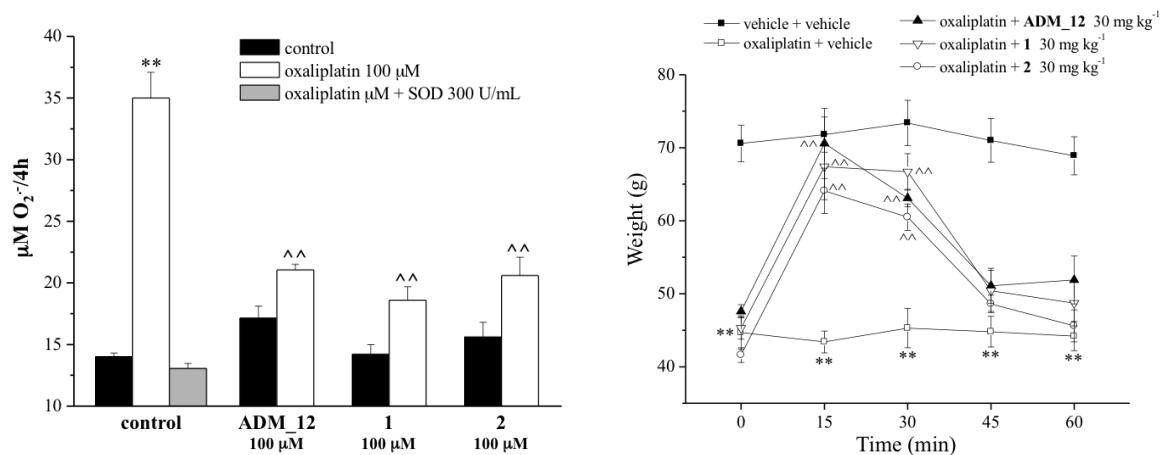
Figure 2. (A) SOD-inhibitable O_2^- levels in astrocyte cell lines. Astrocytes (5×105 cells/well, 2 control wells and 2 wells pre-treated with **ADM_12**, **1** or **2**) were exposed to 100 μM OXA for 4h. The effect of 100 μM **ADM_12** co-incubation on SOD-inhibitable superoxide anion O_2^- on levels are depicted. The non-specific absorbance measured in the presence of SOD was subtracted to the total value. Values are expressed as mean ± s.e.m. of 3 experiments. **P < 0.01 *vs*. control and ^^P < 0.01 vs OXA treatment. (B) OXA-induced neuropathic pain: anti-hypersensitive effect of **ADM_12** in comparison to **1** and **2**. Rats were daily treated i.p. with 2.4 mg kg-1 oxaliplatin (in 0.5% glucose solution). The response to a noxious mechanical stimulus was evaluated on day 21 by the Paw-pressure test. Vehicle (1% CMC) or 30 mg kg-1 **ADM_12**, **1** or **2** were administered p.o., measurements were performed over time. Each value represents the mean ± S.E.M. of 12 rats per group, performed in two different experimental sets. *^P<0.01 *vs*. vehicle + vehicle; ^^P<0.01 *vs* oxaliplatin + vehicle

Antihyperalgesic properties. To evaluate the pain-relieving property of the tested compounds, a painful neuropathic condition was reproduced in rats with a repeated treatment with OXA (2.4 mg kg^{-1}, i.p., daily). On day 21, the pain threshold was measured by the paw pressure test

applying a noxious mechanical stimulus. Oxaliplatin-treated animals showed (Figure 2B) a decreased threshold reported as a reduced weight tolerated on the paw (44.7 ±2.3 g in comparison to 70.6 ± 2.5 g of control animals). **ADM_12**, acutely administered p.o. (30 mg kg^{-1}) counteracted the OXA-induced hypersensitivity taking effect 15 min after treatment. A complete reversion of pain lasted up to 75 min. A similar profile was observed for compounds **1** and **2** (Figure 2B) even though a complete reversion of the noxious effect is observed only with **ADM_12**.

Inhibition of TRPA1 activated with OXA. As reported,[9] **ADM_12** is able to inhibit TRPA1 methanol- and AITC-evoked current with a low micromolar constant. Thus, using the patch clamp technique, we investigated the effect of **ADM_12** on TRPA1 evoked current by OXA. After perfusion of OXA 50 μM we observed the activation of TRPA1 channel, which is rapidly and completely reverted in the presence of **ADM_12** 30 μM. The corresponding time courses (Figure 3) and III curves (Figure S2, Supporting Information) are reported (see Table S1 and Figure S1 for details about compounds **1** and **2**).
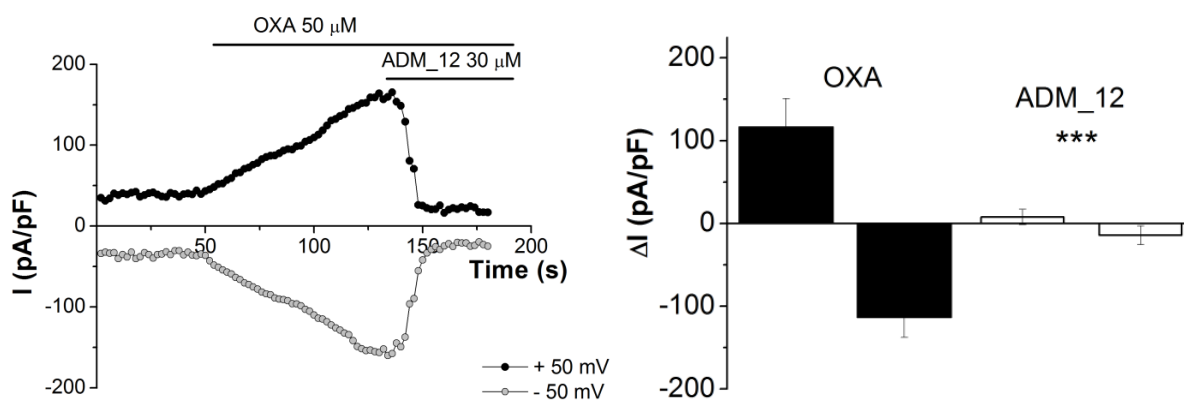

Figure 3. (A) Time course obtained from voltage ramps measured at +50 mV (black circles) and -50 mV (grey circles). OXA (50 μM) and **ADM_12** (30 μM) were applied at the time indicated.

CHO cells were transfected with wild-type TRPA1 channel. (B) Summarized data of TRPA1 whole-cell currents evoked by OXA 50 μM and OXA + **ADM_12** 30 μM (ADM_12). Each column represents mean ± SEM of n = 5 cells. *** p < 0.0001 (unpaired Student's t test).

ADM_12 inhibits carbonic anhydrases IX and XII. Carbonic anhydrases (CAs, EC 4.2.1.1) are zinc metallo-enzymes that catalyze the hydration of carbonic dioxide, producing bicarbonate and protons.[15,16] CA IX is a trans-membrane enzyme up-regulated in many cancer types and playing an important role in the acidification of the outer microenvironment under hypoxia, a hallmark of many tumors.[17] The involvement of CA IX to acidification of the tumor environment has been correlated with the acquisition of metastatic phenotypes and is related to a decrease in the success of anticancer drugs.[18] Recently, some of us reported on the nanomolar *h*CA IX and *h*CA XII inhibitor **8** (see Figure 1), presenting a sulfonic acid residue involved in the binding to the CA IX active site by anchoring to the zinc-coordinated water molecule.[10] Of note, currently a sulfonamide CA IX inhibitor completed phase I clinical trials for the treatment of advanced stage solid tumors and is scheduled for Phase II trials.[19] Keeping in mind the specific CA inhibition mechanism of **8** we investigated **ADM_12** as a possible ligand for CA IX and CA XII. In fact, even though the properties of **ADM_12**, **1** and **2** as TRPA1 inhibitors or to revert OXAIPN are rather similar, overall the pharmacological profile of **ADM_12** is the most interesting. For this reason, all the following tests have been performed on **ADM_12** selected as a lead molecule. We investigated the CA inhibitory activity of **ADM_12** by applying the stopped flow carbon dioxide hydrase assay (Supporting Information), in comparison to acetazolamide (**AAZ**) as standard CA inhibitor against the tumor-associated isoforms *h*CA IX and XII (Table 1, see Table S3 for inhibition data *vs.* other *h*CAs). From the data shown in Table 1, **ADM_12** clearly arose as a

good hCA IX and hCA XII inhibitor, with K_I ranging in high nanomolar range (respectively 653.7 and 727.5 nM). Such results ascribed to **ADM_12** are lower in efficacy than the clinically used **AAZ**, but improved compared to derivative **8**. Anyhow, it should be stressed that the sulfonate derivative **8** derives from the CA-mediated hydrolysis of the corresponding sulfocoumarin, necessary to generate the active species from the original prodrug.[10] Conversely, such activation was not necessary in the case of **ADM_12**, which can directly bind the active site pocket.

Table 1. Inhibition data of human CA isoforms hCA IX and XII with **ADM_12**, compound **8** and the standard sulfonamide inhibitor acetazolamide (**AAZ**) by a stopped flow CO_2 hydrase assay.

	K_I (nM)[a]	
	hCA IX	hCA XII
ADM_12	653.7	727.5
8[b]	6830	4510
AAZ	25.2	5.7

[a]Mean from 3 different assays, by a stopped flow technique (errors were in the range of ± 5-10 % of the reported values). [b] Ref. S7

Molecular modelling. In order to fully explore the binding interaction of the sulfonate derivative **ADM_12** within CA active site, we undertook docking studies taking into consideration the tumor-associated isoform hCA IX. At present, only one X-ray structure of a sulfonate compound within CA is available in Protein Data Bank, that is the adduct of derivative **8** with a modified hCA II (PDB 4BCW).[10] This structure, also referred as hCA II/IX mimic, concerns an engineered protein in which two amino acid mutations are present in the hCA II active site, namely A65S and N67Q, being serine and glutamine the corresponding amino acids found in hCA IX. The

sulfonate group of **8**, which as previously mentioned comes from the CA-mediated hydrolysis of the corresponding sulfocoumarin,[10] was found to anchor to the Zn-coordinated water molecule, differently from compounds containing the sulfonamide moiety that instead directly coordinates to the Zn ion.[20] Considering that **ADM_12** was assayed in vitro against hCA IX (K_I = 653.7 nM), the target used in such experiments was prepared superposing 3IAI (hCA IX) and 4BCW (hCA II/IX mimic) through the Zn ion and the backbone of H94, H96, H119 residues, then joining together only the enzyme 3D coordinates of 3IAI and the catalytic Zn coordinated OH/H_2O group of 4BCW. We report herein only the results obtained for the isomer R, as the stereo-center is located at the outer rim of the aliphatic tail of the molecule and barely affects the poses arisen from the docking studies, thus the highlighted binding mode. Taking as driving principle in the selection of the docking solutions the position of the sulfonate group in the X-ray solved structure, three rather iso-energetic poses were selected, all characterized by not high values of the scoring function (Figure 4 and 5).
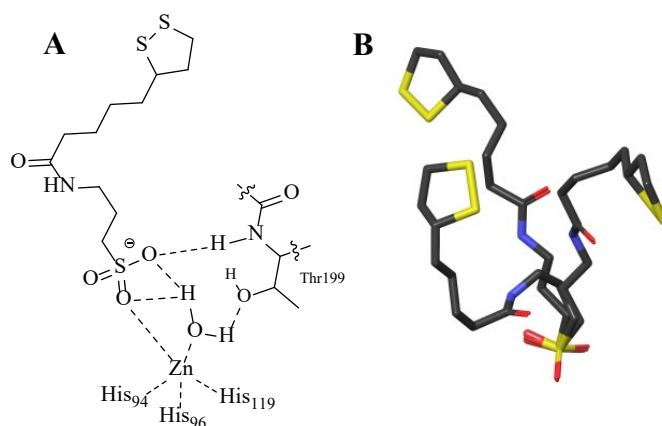

Figure 4. (A) Diagram of the H-bond network the sulfonate moiety is involved in within the active site cavity. (B) Superimposition of the three found orientations of **ADM_12** within hCA IX active site.

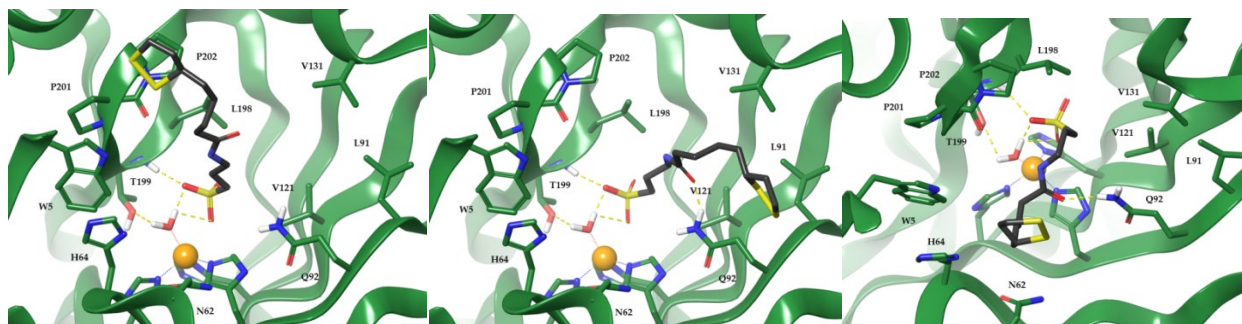A   B   C

Figure 5. Simulated binding modes of compound **ADM_12** within *h*CA IX active site (PDB ID 3IAI): three diverse orientations are shown in panels (A), (B) and (C). The hydrogen bonds are shown as yellow dashed lines.

In the three different poses the sulfonate group was always found to be involved in a wide network of H-bonds (Figure 4A). In particular, two oxygen atoms of the sulfonate moiety accepted a H-bond from the Zn-bound water molecule, which in turn donate an additional one to OG1 oxygen of T199 side chain. Furthermore, one of these sulfonate O atoms established a H-bond with the backbone NH of T199, whereas the other one might be consider as "half-coordinated" to the Zn ion. The three **ADM_12** poses are differentiated by the position of lipoic tail within the binding site cavity (Figure 4B) and each is characterized by hydrophobic contacts involving the propylenic linker and the lipoic moiety which respectively interact with L198, P201, P202 (Figure 5A), V121, L91, V131, Q92 (Figure 5B) and V121, W5, H64, N62 (Figure 5c). Moreover, the amidic carbonyl of the conformers in Figure 5B and Figure 5C is at H bond distance with Q92.

ADM_12 reduces CA IX-mediated acidosis. Recently, in order to analyze the role of CA IX in cancer cells motility, we investigated the extracellular pH in normoxia in extracted human prostate fibroblasts (HPFs) from healthy individuals affected by prostate hyperplasia, cancer-

associated fibroblasts (CAFs) and in prostate cancer (PCa) cells after the treatment with conditioned medium (CM) from HPFs or CAFs.[21] The contact of CAFs with PCa cells gives rise to an increase in extracellular acidity ascribed to CA IX and suggesting that the conditioning loop among stromal and cancer cells involved in cancer cells malignancy and aggressiveness also takes account for acidification of tumor microenvironment. In Figure 6A we report on the effect of **ADM_12** on alkalinisation of extracellular pH in HPFs and CAFs. Fibroblasts were grown to sub-confluence and serum starved for 48h in the presence of **ADM_12**; at the end of incubation, the pH of culture medium was immediately measured by pH meter. We observed that the administration of **ADM_12** unambiguously reduces extracellular acidification confirming a key role of CA IX in this phenomenon.
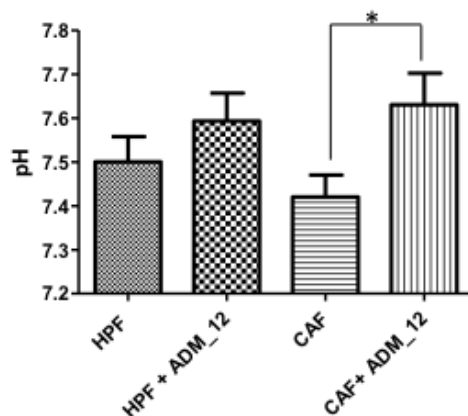

Figure 6. Measure of extracellular pH in HPF and CAF. Cells were serum starved and treated with 100 μM of **ADM_12** for 48h. *p < 0,05 *vs.* CAF.
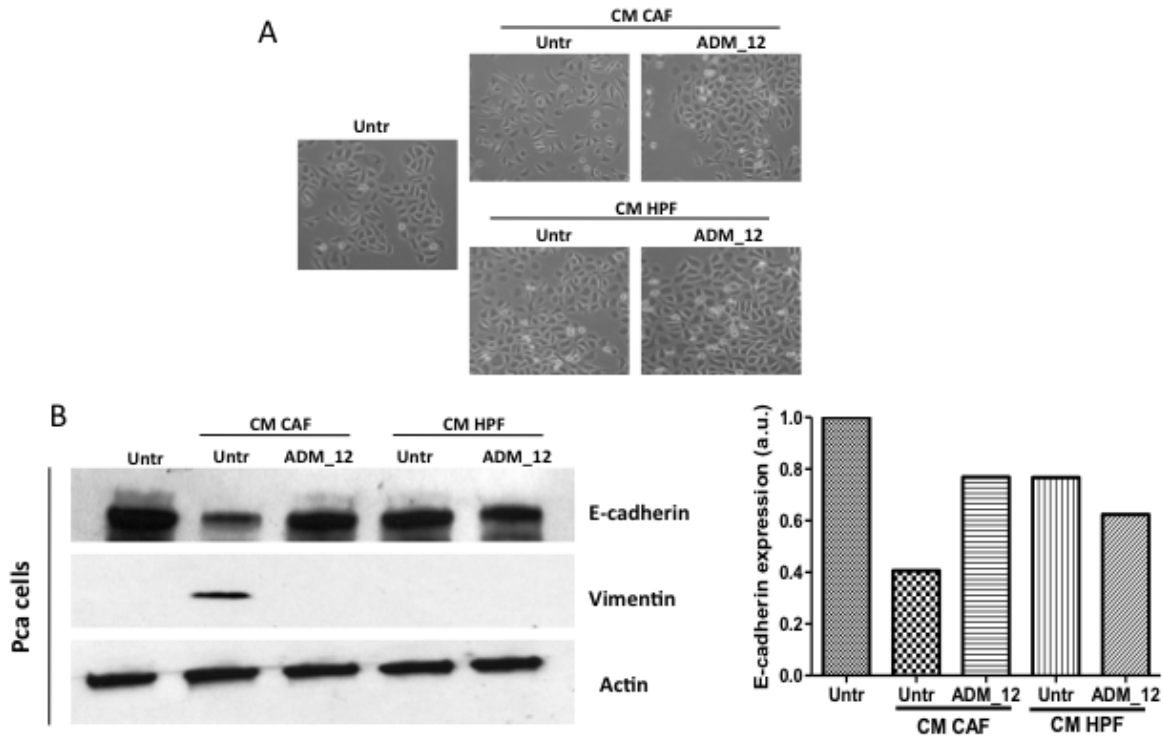
Figure 7. A) HPF and CAF were treated with 100 μM of **ADM_12** for 48 h and CM were harvested. PCa cells were then treated with serum free medium or different CM for 72 h, and then were photographed (B) Left: evaluation of E-cadherin and Vimentin in the same experimental setting described in A. (B) Right: actin immunoblot was used for normalization. Cadherin expression was shown in bar graph, a.u., arbitrary units.

ADM_12 positively interferes in the epithelial-mesenchymal transition (EMT) and invasiveness in PCa cells. A specific role is played by CA IX in the regulation of EMT of cancer cells, a key epigenetic program associated with increased motility, survival and stemness.[21] In particular, we demonstrated that PCa cells undergo EMT in response to their contact with stromal fibroblasts expressing CA IX.[21] Here, we report on the effect of **ADM_12** on CAF-mediated EMT. PCa cells were treated for 72h with conditioned medium (CM) obtained from HPFs and CAFs in the presence or not of **ADM_12**. We

observed that the use of the compound is active in impairing EMT in cancer cells due to CAFs contact, (Figure 7A) preventing the elongation of the cells, as well as the expression of known EMT markers, as E-cadheirn decrease and up-regulation of Vimentin (Figure 7B).
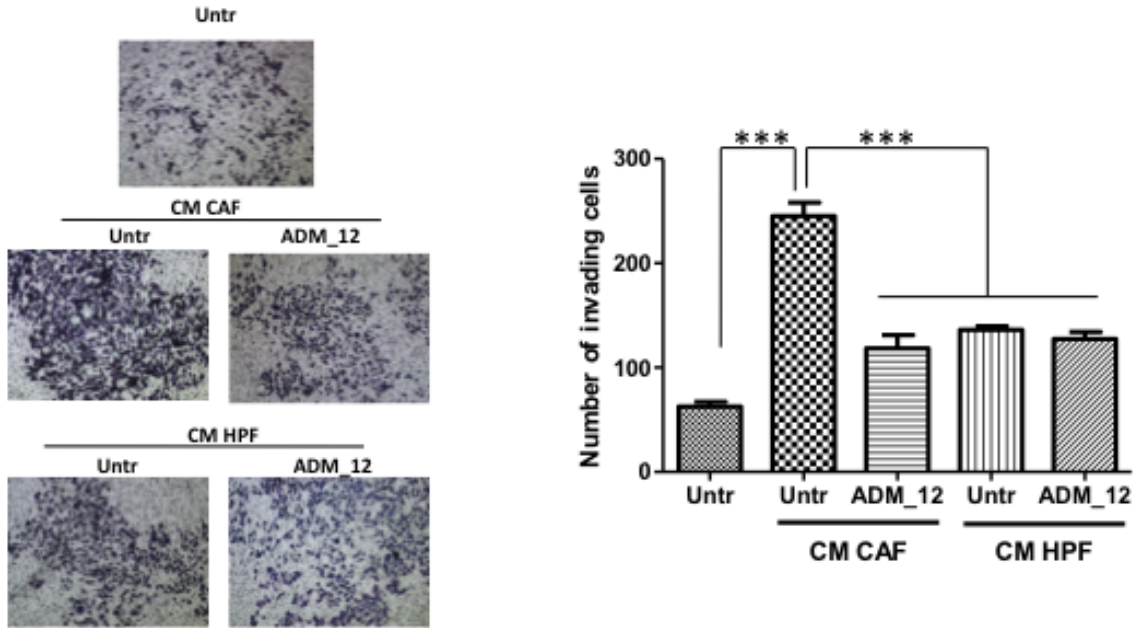

Figure 8. Left: invasion analysis of Pca cells after treatment for 24h with different CM obtained from HPF or CAF (control or in presence of **ADM_12**). Right: bar graph represents the mean of invading cells. ***** < 0,001 *vs*. untreated CAF.**

In keeping with morphological features, **ADM_12** clearly affects invasiveness of cancer cells. We finally treated cells with CM from fibroblasts in the presence or not of **ADM_12** and assayed for their ability to invade through reconstituted matrigel barrier. Our data revealed that the ability of CAFs to elicit a pro-invasive behaviour of cancer cells is severely impaired during the administration of **ADM_12** (Figure 8).

ADM_12 is a MMPs-inhibitor. As above discussed, stromal CA IX leads to extracellular acidification. Since the sensitivity of MMPs to acidity is acknowledged and the key role played by CA IX in MMP-2 and MMP-9's secretion by CAFs is documented,[21] we reasoned that, given the similar active-site topology of MMPs and CAs, it would be worthy to investigate the binding properties of **ADM_12** vs. MMPs. Human matrix metalloproteinase 12 (MMP-12) has been used as representative model of the whole protein family to analyze the structural basis for the interaction of MMPs with the investigated scaffold.[22] To determine the binding affinity of **ADM_12** for the catalytic domain of MMP-12, we analyzed the alteration of the chemical shifts observed in 2D ^{1}H-^{15}N HSQC spectra of the protein upon the titration with the lipoic acid derivative. Several residues forming the S1' cavity, and two zinc binding histidines experience a sizable chemical shift variation at submillimolar concentration (see Figure 9). The fit of the experimental data has provided a dissociation constant of 875 ± 78 µM.[22] The uncommon structure of **ADM_12** as a MMP inhibitor deserved a more accurate investigation. Thus, a detailed structural characterization of the complex MMP-12-**ADM_12** by X-ray diffraction was carried out to investigate the binding mode and the involvement of the catalytic zinc in ligand binding. To confirm the structural data obtained, compound **7** (see Scheme 1) was synthesized and X-ray diffraction of the complex MMP-12-**7** performed. Compound **7** preserves the lipoic portion but presents a propyl alcohol replacing the propyl sulfonate residue of **ADM_12** (Scheme 1).
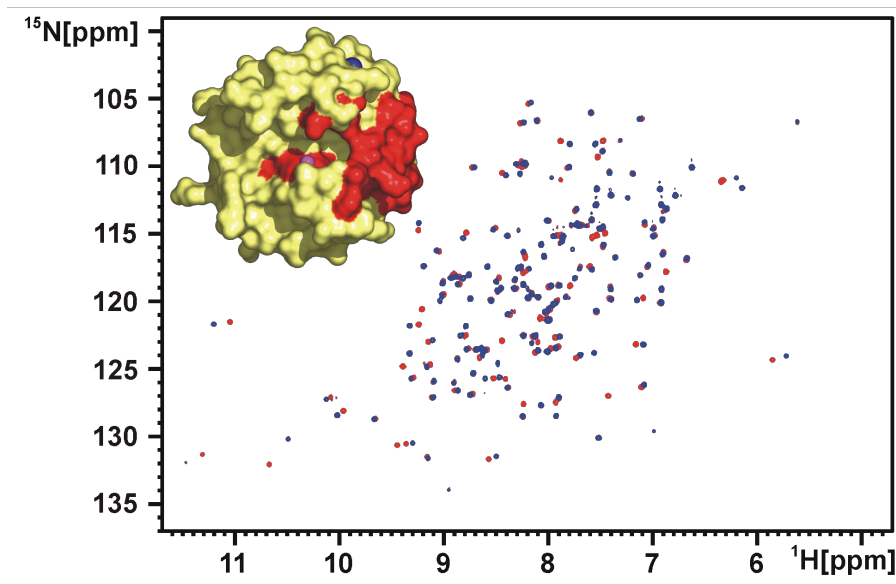
Figure 9. ^{1}H-^{15}N HSQC spectrum of the catalytic domain of MMP-12 in the absence (red) and presence of ADM_12 (3.3 mM) (blue), with the surface model of MMP-12 showing in red the residues experiencing the largest chemical shift variation.

Binding of ADM_12 and 7 are non-zinc binding ligands of MMP-12. In both structures, AHA (hydroxamic acid, see Supporting Information) is not displaced by **ADM_12** or **7** and it shows its typical binding to the catalytic zinc at full occupancy:[23] it chelates zinc with the two oxygens and it establishes hydrogen bond interactions with the backbone of A182, with the carboxylate of the catalytic E219 and with H228. The above necessarily implies that the two lipoic-containing ligands do not interact directly with the catalytic zinc. Furthermore, they establish one interaction only with AHA namely a relatively weak hydrogen bond between one of the two oxygens of AHA and the carbonyl oxygen present in the middle of the chain of the ligands (Figure 10). Both ligands bend similarly upon binding to the protein in such a way that the part containing the heterocycle is accommodated into the S1' pocket while the chain occupies the groove which is normally occupied by the substrate prior to its hydrolysis. The electron density of the lipoic-

containing ligands appears of good quality in both cases supporting their full occupancy; in particular, it shows that the heterocyclic portion of both, **ADM_12** and **7**, containing a disulfide bridge remains closed, witnessing that the bridge is not reduced. In the case of the sulfonate ligand, **ADM_12**, the two sulfur atoms of the ring into the S1' pocket are placed at 3.65 Å from the carbonyl oxygens of V235 and F237. In the case of the OH ligand (compound **7**) the ring is slightly tilted so that the two sulfur atoms are at 3.6 Å from the carbonyl oxygens of T239 and K241. As already mentioned, the amidic carbonyl oxygen points towards AHA whereas the hydroxyl group of **7** and the sulfonate of **ADM_12**, protrude outside the molecule towards the solvent. In the case of **ADM_12** the sulfonate moiety is stabilized by two strong hydrogen bond interactions between two of the three oxygens of the ligand and G179 and Y240.
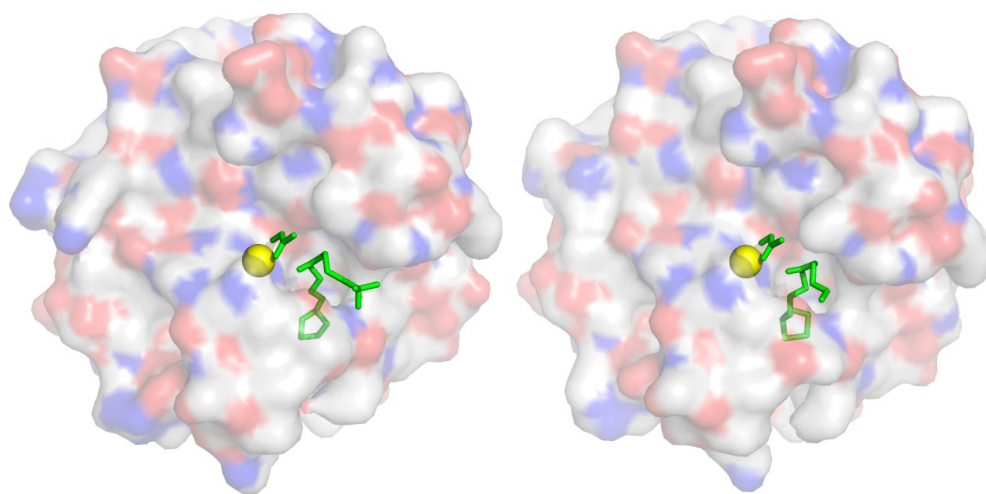

Figure 10. View of the interaction of **ADM_12** (left panel, pdb code 5N5J) and **7** (right panel, pdb code 5N5K) with MMP-12. The two ligands and AHA are represented as green sticks, the protein as transparent surface and the catalytic zinc as yellow sphere.

DISCUSSION AND CONCLUSION

So far, OXA is the chemoterapic commonly used to treat colon-rectal and resistant prostate cancer. However, the oxidative stress triggered by OXA induces a neuropathy which is considered the neuropathic pain the most difficult to treat. In this manuscript, we showed the properties of **ADM_12** to revert OXAIN in an experimental animal model and we proved **ADM_12** effective in reducing cancer cells invasiveness by inhibiting CA IX. **ADM_12**, formed by a lipoic acid residue linked to the homotaurine, has a remarkable safe profile in terms of cells viability and cardiotoxicity.[9] In order to exclude a possible effect of the distance between the cyclic disulphide and the sulfonic acid tail on the biological properties of **ADM_12**, the lower homologue **1** and the higher homologue **2** were synthesized The lipoic portion of **ADM_12** reasonably accounts for the antioxidative properties we assessed *in vitro* (NBT test, Table S2 and astrocytes cell culture Figure 2). *In vivo*, **ADM_12**, administered to rat previously treated with OXA, completely counteracted the OXA-induced hypersensitivity (see Figure 2B). The oxidative stress caused by OXA is also known to trigger the activation of TRPA1 channel evoking a noxious stimolous;[7] we confirmed **ADM_12** an efficient inhibitor of TRPA1,[9] able to completely revert the OXA-induced activation of the channel (Figure 3). The two homologues and **ADM_12**, namely **1** and **2**, showed similar antioxidative properties, close effects as TRPA1 inhibitors as well as in *in vivo* tests. This allows to exclude any effect due to the distance between the disulphide bridge and the sulfonic acid portion.

The functional contribution of CA IX to specific biological processes critical for cancer progression, including pH regulation, migration and invasion, provide the rational for its use as relevant therapeutic target.[22] In 2015 it was published the first example of CA IX inhibitor characterized by a sulfonate residue (see compound **8**, Figure 1). Considering the structural features of **ADM_12**, we investigated its binding affinity *vs.* CA IX and CA XII, both involved in

cancer progression. Tests of inhibition *vs. h*CA IX and *h*CA XII clearly showed a high nanomolar affinity of **ADM_12** for both the CAs (Table 1). The binding interactions of the sulfonate **ADM_12** with the CA active site, explored running computational studies, allowed to properly rationalize the good inhibition constants assessed. We confirmed these inhibition properties by testing **ADM_12** in CA IX-mediated biochemical processes. In particular, we observed that the administration of **ADM_12** reduces extracellular acidification and clearly impair EMT in cancer cells (Figure 7), preventing the expression of ETM markers and reducing invasiveness of cancer cells (Figure 8). The binding properties of **ADM_12** *vs.* the acidity sensitive MMP-2 and MMP-9 were also examined. The chemical shifts recorded by 2D ^{1}H-^{15}N HSQC spectra of MMP-12 (model for the MMPs family) upon the titration with **ADM_12** provided a high micro molar K_d. X-ray diffraction, carried out to investigate the binding mode of **ADM_12**, showed that it is a non-zinc binding ligand of MMP-12.

Concluding, the simple structure of **ADM_12** collects unique biological properties: *i)* blocks OXA-induced TRPA1 current, *ii)* reverts *in vivo* OXAIN, *iii)* inhibits CA IX and CA XII, two CAs involved in tumor progression and *iv)* impairs EMT and invasiveness in cancer cells. The unique properties of **ADM_12** and the soundness of the data reported could represent a glimmer in the dark scenario exposed to cancer patients suffering from the side effects related to the chronic administration of chemotherapy and from the intractable neuropathic pain induced by chemotherapy.

EXPERIMENTAL SECTION

Materials. Patch-clamp studies were carried out in Chinese Hamster Ovary (CHO) cells transiently expressing TRPA1 channel. For heterologous protein expression, cells were plated in

6-wells cell culture dishes with 2 ml growth medium, 24 h before transfection. Cells were transiently transfected using X-tremeGENE 9 transfection reagent (Roche), according to the protocol supplied by the manufacturer. EGFP fluorescence was used as marker of successful transfection. Electrophysiology studies were performed 48-72 h after transfection.

Male Sprague-Dawley (SD) rats (Harlan, Varese, Italy) weighing approximately 200 to 250 g at the beginning of the experimental procedure were used. Pirc (F344/NTac-Apc[am1137]) rats, originally obtained from Taconic (Taconic Farms, Inc. USA) were bred in CESAL (Centro Stabulazione Animali da Laboratorio, University of Florence, Italy) in accordance with the Commission for Animal Experimentation of the Italian Ministry of Health. Animals were housed in CeSAL and used at least 1 week after their arrival.

Synthesis of compounds 1 and 2. General procedure. The activated lipoic acid **3** in DMF/H_2O as solvent was treated at room temperature with the aminosulfonic derivative **4**[S24] or **5** to afford after purification by column chromatography on silica gel the derivative **1** (60%) or **2** (80%) respectively, obtained as sodium salt. Compound **1**: Column chromatography on silica gel (eluent: CH_2Cl_2/MeOH 4/1; 5/2). Glassy solid; ^{1}H-NMR (500 MHz, D_2O): δ 3.67-3.62 (m, 1H, C*H*-3), 3.53-3.50 (t, ^3J(H,H)=6.8 Hz, 2H, C*H$_2$*-10), 3.22-3.12 (m, 2H, C*H$_2$*-1), 3.06-3.02 (t, ^3J(H,H)=6.8 Hz, 2H, C*H$_2$*-9), 2.46-2.41 (m, 1H, C*H*-2'), 2.23-2.20 (m, 2H, C*H$_2$*-7), 1.95-1.91 (m, 1H, C*H*-2), 1.73-1.56 (m, 3H), 1.40-1.36 ppm (m, 3H). ^{13}C-NMR (125 MHz, D_2O): δ 176.8, 56.5, 49.8, 40.3, 38.1, 35.5, 35.0, 33.7, 27.9, 24.9 ppm. HRMS calculated for $C_{10}H_{18}NO_4S_3^-$ [M-H]$^-$: 312.03980; found: 312.03923. Elemental Anal. ($C_{10}H_{18}NNaO_4S_3$) calculated: C, 35.81; H, 5.41; N, 4.18; found: C, 35.78; H, 5.54; N, 4.46. Compound **2**: Column chromatography on silica gel (eluent: CH_2Cl_2/MeOH 4/1; 5/2). Glassy solid; ^{1}H-NMR (500 MHz, D_2O): δ 3.68-3.63 (m,

1H, CH-3), 3.20-3.12 (m, 4H, CH_2-1, CH_2-12), 2.88-2.85 (m, 2H, CH_2-9), 2.46-2.42 (m, 1H, CH-2), 2.21-2.18 (m, 2H, CH_2-7), 1.96-1.92 (m, 1H, CH-2'), 1.72-1.67 (m, 3H), 1.59-1.57 (m, 5H), 1.40-1.35 (m, 2H). ^{13}C-NMR (125 MHz, D$_2$O): δ 176.8, 56.5, 50.6, 40.3, 38.8, 38.1, 35.6, 33.7, 27.8, 27.4, 25.1, 21.6 ppm. HRMS cald for C$_{12}$H$_{22}$NO$_4$S$_3^-$ [M-H]$^-$: 340.07110; found: 340.07008. Elemental Anal. (C$_{12}$H$_{22}$NNaO$_4$S$_3$) calculated: C, 39.65; H, 6.10; N, 3.85; found: C, 39.58; H, 6.32; N, 4.05.

Synthesis of compound 7. A solution of amino alcohol **6** (390 mg, 5.19 mmol) in DMF/H$_2$O was treated at room temperature with solid NaHCO$_3$ (5.19 mmol) then cooled to 0 °C. A solution of **3** (1.5 g, 4.94 mmol) in DMF was added and the reaction mixture warmed to room temperature and stirred overnight. Water (100 mL) is then added to the mixture and the organic layer extracted with EtOAc (2x). The crude (1.4 g) was purified by column chromatography on silica gel (eluent MeOH/DCM-8/1) to afford **7** as waxy solid (770 mg, 60%). Column chromatography on silica gel (eluent: CH$_2$Cl$_2$ with 8% MeOH). Waxy solid; ^{1}H-NMR (500 MHz, CDCl$_3$): δ 6.30 (bs, 1H, NH), 3.64-3.61 (m, 2H, CH_2-11), 3.59-3.54 (m, 1H, CH-3), 3.41-3.38 (m, 2H, CH_2-9), 3.27 (bs, 1H, OH), 3.20-3.09 (m, 2H, CH_2-1), 2.49-2.43 (m, 1H, CH-2), 2.24-2.18 (m, 2H, CH_2-7), 1.49-1.87 (m, 1H, CH-2'), 1.75-1.60 (m, 6H), 1.52-1.42 ppm (m, 2H). ^{13}C-NMR (125 MHz, CDCl$_3$): δ 174.1, 59.4, 56.4, 40.3, 38.5, 36.4, 36.4, 34.6, 32.2, 28.9, 25.5 ppm. HRMS cald for C$_{11}$H$_{22}$NO$_2$S$_2^+$ [M+H]$^+$: 264.10920; found: 264.10903. Elemental Anal. (C$_{11}$H$_{21}$NO$_2$S$_2$) calculated: C, 50.16; H, 8.04; N, 5.32; found: C, 50.08; H, 8.30; N, 5.02.

ASSOCIATED CONTENT

Supporting Information

^{1}H and ^{13}C spectra for compounds **1**, **2** and **7**, *in vitro* and *in vivo* methods, *h*CAs inhibition, NMR spectroscopy, X-ray data. The following files are available free of charge.

PDB codes: 5N5J for **ADM_12** and 5N5K for **7**.

AUTHOR INFORMATION

Corresponding Authors

*E-mail: cristina.nativi@unifi.it. Phone (+39)0554573540; claudiu.supuran@unifi.it.

Notes

The authors declare no competing financial interest.

Authors will release the atomic coordinates and experimental data upon article publication.

REFERENCES

(1) Woolf C.J.; Mannion R.J.; Neuropathic pain: aetiology, symptoms, mechanisms and management. *Lancet*, **1999**, *353*, 1959-1964.

(2) Majithia, N.; Loprinzi, C.L.; Smith, T.J.; New practical approaches to chemotherapy-induced neuropathic pain: prevention, assessment and treatment. *Oncology,* **2016**, *30*, 1020-29.

(3) Grothey, A.; Clinical management of oxaliplatin-associated neurotoxicity. *Clin. Colorectal Cancer,* **2005**, *1*, S38-46.

(4) Hoshino, H.; Hida, K.; Ganeko, R.; Sakai, Y.; Goshajinkigan for reducing chemotherapy induced periphereal neuropathy: protocol for a systematic review and meta-analysis. *Int. J. Colorectal Dis.,* **2016**, DOI 10.1007/s00384-016-2727-y.

(5) Argyriou, A.A.; Bruna, J.; Marmiroli, P.; Cavalletti, G.; Chemotherapy-induced peripheral neuropathy: an update. *Crit. Rev. Oncol. Hematol.,* **2012**, *82*, 51-77.

(6) Zhao, M.; Isami, K.; Nakamura, S.; Shirakawa, H.; Nakagawa, T.; Kaneko, S.; Acute cold hypersensitivity characteristically induced by oxaliplatin is caused by the enhanced responsiveness of TRPA1 in mice. *Mol. Pain*, **2012**, *8*, 55.

(7) Nassini, R.; Gees, M.; Harrison, S.; De Siena, G.; Materazzi, S.; Moretto, N.; Failli, P.; Preti, D.; Marchetti, N.; Cavazzini, A.; Manicini, F.; Pedretti, P.; Nilius, B.; Patacchini, R.; Geppetti, P.; Oxaliplatin elicits mechanical and cold allodynia in rodends via TRPA1 receptors stimulation. *Pain*, **2011**, *152*, 1621-31.

(8) Nativi, C.; Gualdani, R.; Dragoni, E.; Di Cesare Manneli, L.; Sostegni, S.; Norcini, M.; Gabrielli, G.; la Marca, G.; Richichi, B.; Francesconi, O.; Moncelli, M.R.; Ghelardini C.; Roelens, S.; A TRPA1 antagonist reverts oxaliplatin-induced neuropathic pain. *Sci. Rep.,* **2005**, *3*, DOI: 10.1038/srep02005.

(9) Gualdani, R.; Ceruti, S.; Magni, G.; Merli, D.; Di Cesare Manneli, L.; Francesconi, O.; Richichi, B.; Francesconi, O.; la Marca, G.; Ghelardini, C.; Moncelli, M.R.; Nativi C.; Lipoic-based TRPA1/TRPV1 antagonist to treat orofacial pain. *ACS Chem. Neurosci.,* **2015**, *6*, 380-385.

(10) Grandane, A.; Tanc, M.; Di Cesare Mannelli, L.; Carta, F.; Ghelardini, C.; Zalubovskis R.; Supuran, C.; 6-Substituted sulfocumarins are selective carbonic anhydrase IX and XII inhibitors with significant cytotoxicity against colorectal cancer cells. *J. Med. Chem.* **2015**, *58*, 3975-83.

(11) Gauchan, P.; Andoh, T.; Kato A.; Kuraishi, Y.; Involvement of increased expression of transient receptor potential melastin 8 in oxaliplatin-induced cold allodynia in mice. *Neurosci. Lett.,* **2009**, *458*, 93-95.

(12) Descoeur, J.; Pereira, V.; Pizzoccaro, A.; Francois, A.; Ling, B.; Maffre, V.; Couette, B.; Busserolles, J.; Courteix, C.; Noel, J.; Lazdunski, M.; Eschalier, A.; Authier N.; Bourinet, E.; Oxaliplatin-induced cold hypersensivity is due to remodeling of ion channel expression in nociceptors. *EMBO Mol. Med.,* **2011**, *3*, 266-278.

(13) Di Cesare Mannelli, L.; Pacini, A.; Bonaccini, L.; Zanardelli, M.; Mello T.; Ghelardini, C.; Morphologic features and glial activation in rat oxaliplatin-dependent neuropathic pain. *J. Pain,* **2013**, *14*, 1585-600.

(14) Di Cesare Mannelli, L.; Pacini, A.; Micheli, L.; Tani, A.; Zanardelli, M.; Ghelardini, C.; Glial role in oxaliplatin-induced neuropathic pain. *Exp Neurol*., **2014**, *261*,22-33.

(15) Supuran, C.T.; Carbonic Anhydrase: novel therapeutic applications for inhibitors and activators. *Nature Rev Drug Discov.,* **2008**, *7*, 168-81.

(16) Neri D.; Supuran, C.T.; Interfering with pH regulation in tumor as a therapeutic strategy. *Nature Rev Drug Discov.,* **2011**, *10*, 767-77.

(17) Swietach, P.; Hulikova, A.; Vanghan-Jones, R.D.; Harries, A.L.; New insight into the physiological role of carbonic anhydrase IX in tumor pH regulation. *Oncogene,* **2010**, *29*, 6509-21.

(18) Tafreshi, N.K.; Lloyd, M.C.; Bui, M.M.; Gillies R.J.; Morse, D.L.; Carbonic anhydrase IX as an imaging and therapeutic target for tumors and metastases. *Subcell Biochem*., **2014**, *75*, 221-54.

(19) Pacchiano, F.; Carta, F.; McDonald, P.C.; Lou, Y.; Vullo, D.; Scozzafava, A.; Dedhar, S.; Supuran, C.T.; Ureido-substituted benzenesulfonamides potently inhibit carbonic anhydrase IX and show antimetastatic activity in a model of breast cancer metastasis *J. Med. Chem.*, **2011**, *54*, 1896−1902.

(20) Alterio, V.; Hilvo, M.; Di Fiore, A.; Supuran, C.T.; Pan, P.; Parkkila, S.; Scaloni, A.; Pastorek, J.; Pastorekova, S.; Pedone, C.; Scozzafava, A.; Monti S.M.; De Simone, G.; Crystal structure of the catalytic domain of the tumor-associated human carbonic anhydrase IX. *Proc. Natl. Acad. Sci. U. S. A.* **2009**, *106*, 16233−38.

(21) Fiaschi, T.; Giannoni, E.; Taddei, M.L.; Cirri, P.; Marini, A.; Pintus, G.; Nativi, C.; Richichi, B.; Scozzafava, A.; Carta, F.; Torre, E.; Supuran C.T.; Chiarugi, P.; Carbonic Anhydrase IX from cancer-associated fibriblastes drives epitelial-mesenchymal transition in prostate carcinoma cells. *Cell Cycle,* **2013**, *12*, 1791-1801.

(22) Winter, A.; Sigurdardottir, A.G.; Di Cara, D.; Valenti, G.; Blundell T.L.; Gherardi, E. Developing antagonists for theMet/HGF/SF protein-protein interaction using a fragment-based approach. *Chem Sci*., **2015**, *6*, 6147-57.

(23) Udi, Y.; Fragai, M.; Grossman, M.; Mitternacht, S.; Arad-Yellin, R.; Calderone, V.; Melikian, M.; Toccafondi, M.; Berezovsky, I.N.; Luchinat, C.; Sagi, I.; Unraveling hidden regulatory sites in structurally homologous metalloproteinases. *J. Mol Biol.,* **2013**, *425*, 2330-46.

(24) Deng, H.; Liu, X.; Xie, J.; Yin, R.; Huang, N.; Gu Y.; Zhao, J.; Quantitative and site-directed chemical modification of hypocrellins toward direct drug delivery and effective photodynamic activity. *J. Med. Chem.,* **2012**, *55*, 1910-19.

TABLE OF CONTENT
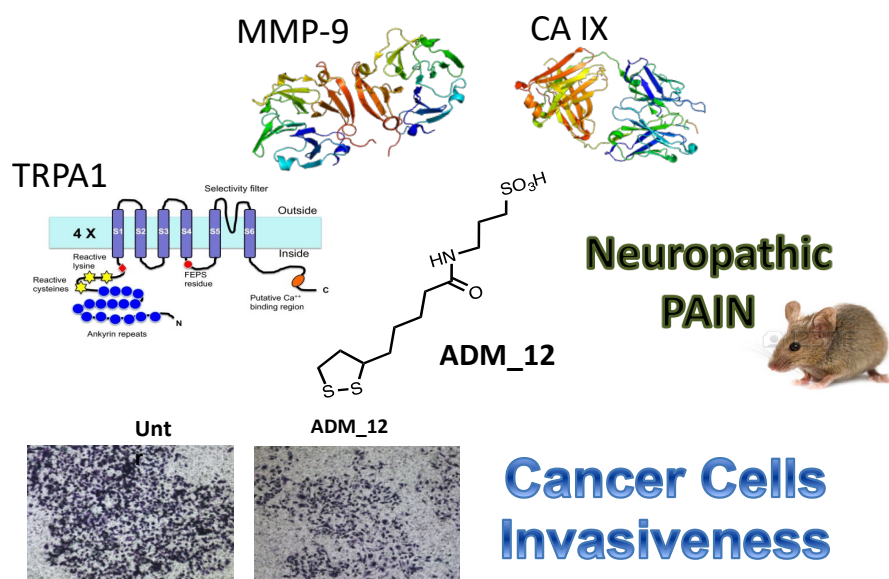
The analgesic **ADM_12** reverts Oxaliplatin-induced neuropathic pain and reduces cancer cells aggressiveness.

BRIEF: A lipoyl-homotaurine derivative reverts oxaliplatin-induced neuropathic pain and reduces cancer cells aggressiveness.